Universiteit
Leiden
The Netherlands

Targeting MHC-I related proteins for cancer diagnosis and therapy

Verhaar, E.R.

Citation
Verhaar, E. R. (2024, July 4). *Targeting MHC-I related proteins for cancer diagnosis and therapy*. Retrieved from https://hdl.handle.net/1887/3766089

Version:	Publisher's Version
License:	Licence agreement concerning inclusion of doctoral thesis in the Institutional Repository of the University of Leiden
Downloaded from:	https://hdl.handle.net/1887/3766089

Note: To cite this publication please use the final published version (if applicable).

Chapter 5:

Nanobody-based CAR NK-92 cells for possible immunotherapy of MICA⁺ tumors

Elisha R. Verhaar[1,2], Willemijn J.C. van Keizerswaard[1], Anouk Knoflook[1], Thomas Balligand[1], Hidde L. Ploegh[1,2]

[1]Program in Cellular and Molecular Medicine, Boston Children's Hospital, Harvard Medical School, Boston, MA 02115, USA
[2]Department of Cell and Chemical Biology, Leiden University Medical Centre, Leiden, The Netherlands

PNAS Nexus
2024 May:3(5)
DOI: 10.1093/pnasnexus/pgae184

Abstract

The glycoproteins MICA and MICB are upregulated on the surface of cells undergoing stress, for instance due to (viral) infection or malignant transformation. MICA/B are the ligands for the activating receptor NKG2D, found on cytotoxic immune cells like NK cells, $CD8^+$ T cells, and γδ T cells. Upon engagement of NKG2D, these cells are activated to eradicate the MICA/B-positive targets, assisted by the secretion of cytokines. Nanobodies, or VHHs, are derived from the variable regions of camelid heavy-chain only immunoglobulins. Nanobodies are characterized by their small size, ease of production, stability, and specificity of recognition. We generated nanobodies that recognize membrane-bound MICA with high affinity. Here, we use these nanobodies as building blocks for a chimeric antigen receptor (CAR) to establish VHH-based CAR NK cells. These anti-MICA nanobody-based CAR NK cells recognize and selectively kill MICA-positive tumor cells *in vitro* and *in vivo*. We track localization of the VHH-based CAR NK cells to MICA-positive lung metastases by immuno-positron emission tomography (PET) imaging.

Significance statement

MICA is a Class I MHC-related surface glycoprotein, upregulated by virus-infected or malignantly transformed cells. MICA is overexpressed on cancers of hematopoietic and epithelial origin but is absent from healthy cells. We generated nanobodies, the recombinantly expressed variable regions of camelid heavy-chain only immunoglobulins, that recognize MICA with high affinity. We use the nanobodies as building blocks for chimeric antigen receptors (CAR) on NK-92 cells, which recognize and selectively kill $MICA^+$ tumor cells in vitro and in vivo. We track the localization of the nanobody-based CAR NK cells to lung metastases of mice by immuno-PET imaging. The presence of MICA on many tumor types, and absence from healthy tissue, makes it a promising target for cancer immunotherapy.

Introduction

The MHC class I chain-related proteins A and B (MICA and MICB) are surface glycoproteins that are absent from healthy cells but upregulated on malignantly transformed or otherwise stressed human cells[224]. High levels of MICA/B have been reported in cancers of both hematopoietic and epithelial origin[219,224–228]. MICA/B are ligands for the activating receptor NKG2D, found on NK cells, $CD8^+$ T cells, and γδ T cells[218]. Upon engagement of MICA/B with NKG2D, these cytotoxic immune cells are activated to eradicate MICA-positive target [219–221].

The tumor microenvironment (TME) affects surface expression of the ligands of NKG2D transcriptionally and post-translationally. Surface expression of MICA and MICB on tumor cells can be downregulated through shedding, mediated by proteolytic cleavage involving ADAM-type metalloproteases at the MICA α3 domain[236]. Loss of surface-bound MICA renders tumor cells less sensitive to NKG2D-positive NK cells[233,235].

Nanobodies, also known as VHHs, are the variable heavy-chain fragments of camelid-derived heavy-chain only immunoglobulins[301]. Nanobodies are characterized by their small size compared to conventional immunoglobulins (15 kD versus 150 kD), which allows for excellent tissue penetration, stability, solubility, and ease of production[309–311]. Nanobodies are poorly immunogenic and have a short circulatory half-life, making them valuable tools for the construction of PET imaging agents[314,329,380,387,388,419,420], nanobody-drug conjugates[315,386,436], and chimeric antigen receptors in cell-based therapies[210,474–478,546–551].

The latter is based on a cornerstone of immunotherapy known as adoptive cell transfer (ACT), in which immune cells (often the patient's own lymphocytes) are given to a patient as cancer therapy. When using tumor infiltrating lymphocytes expanded ex vivo, this form of treatment is referred to as TIL therapy. In another form of ACT, the patient's T or NK cells are engineered to express a chimeric antigen receptor (CAR) that targets the tumor and exerts cytotoxic activity upon binding to the target recognized by the CAR. In such cells, the CAR dictates the antigen specificity of the cell towards a target of choice. The CAR also contains intracellular signaling domains derived from several proteins such as 4-1BB, CD28, and CD3ζ. These signaling domains activate the CAR cell in response to antigen recognition[579,580] and trigger cytotoxic activity as well as cytokine release. Typically, the antigen recognition domain of the CAR is based on a single-chain variable fragment (scFv), derived from a full-sized immunoglobulin by connecting the variable regions of the immunoglobulin heavy and light chains by means of a short linker into a single construct. The affinity and specificity of scFvs must be carefully compared to that of the source immunoglobulin to maintain its functional properties. When expressed in mammalian cells, domain swaps can lead to self-aggregation of scFv-based CARs[581–584]. The possible immunogenicity of the scFv is a factor to be considered as well. Nanobodies are poorly immunogenic in humans, presumably because of the pronounced homology between camelid and human variable heavy (V_H) chain sequences[196,197].

The FDA has approved several CAR T cell therapies for hematopoietic cancers, such as relapsed or refractory B-cell lymphoma or acute lymphatic leukemia, based on CD19 targeting with an scFv, and relapsed or refractory multiple myeloma, based on CARs that target B-cell maturation antigen (BCMA) via either an scFv or a VHH[585–587], the latter with remarkable clinical efficacy. A major reported side effect of CAR T therapy is cytokine release syndrome, which is systemic inflammation caused by excessive cytokine secretion by the CAR T cells. The cytokines released by NK cells do not induce such inflammation, and thus do not cause cytokine release syndrome[217]. For these reasons, CAR NK cell therapy is potentially a safer alternative to CAR T cell therapy.

CAR NK cells can be produced from a variety of sources: from the patient's or a donor's peripheral blood, from a placenta or from umbilical cord blood, existing immortalized NK cell lines (NK-92) or manufactured from induced pluripotent stem cells (iPSC)[205–210]. Unlike T cells, NK cells do not pose the risk of GVHD in an allogeneic setting. In fact, NK cells are believed to protect against GVHD in other T cell-based cancer treatments[211–215]. Furthermore, NK cells also allow the inclusion of a wider range of co-stimulatory domains, using not only traditional intracellular domains derived from CAR T therapies based on CD28, 4-1BB, and CD3ζ, but also NK-specific domains such as CD244, CD137, and NK-Ars[209,216,217]. If a tumor were to downregulate the CAR's target in an attempt at immune escape, the NK cells might still be effective against the tumor cells because of their intrinsic cytotoxic activity. NK cell-based therapies have entered clinical trials for targeting NY-ESO-1 in synovial carcinoma, myxoid liposarcoma, multiple myeloma, or certain solid tumors. These NK cells are harvested from cord blood and modified with an NY-ESO-1 TCR and IL-15 receptors. Several other pre-clinical studies with CAR NK cells include CARs that target CD19 and CD20 in B cell lymphoma and leukemia[588–595], GD2 in neuroblastoma and breast cancer[596–598], and HER2 in breast cancer and other epithelial cancers[599,600].

Ideally, the target of CAR immune cells is present only on tumor cells and absent from normal tissue, to reduce unwanted off-target effects. Because MICA is expressed primarily on stressed and cancerous cells, MICA is an appealing target for adoptive cell transfer. We have described the production of MICA-targeting nanobodies, VHH-A1 and VHH-H3. These nanobodies recognize the MICA*008 and *009 alleles with nanomolar affinity and recognize surface-disposed MICA on cancer cells[575].

Here, we use these anti-MICA nanobodies to establish VHH-based CAR NK cells. We show that these CAR NK cells recognize and selectively kill MICA-positive tumor cells *in vitro* and *in vivo*.

Materials and methods

Cell culture

The NK-92 cells were obtained from S.K. Dougan (Dana Farber Cancer Institute). NK-92 cells were cultured in complete αMEM (αMEM; no nucleosides, supplemented with 12.5% horse serum, 12.5% fetal bovine serum (FBS), 2mM L-glutamine, 0.1 M 2-mercaptoethanol, 0.02 mM folic acid, 100 U/mL recombinant IL-2 and 100 U/mL penicillin/streptomycin). B16F10 murine melanoma cells and EL-4 lymphoma cells, and their MICA$^+$ transfectants, were obtained from K. Wucherpfennig (Dana Farber Cancer Institute). HEK293T and B16F10 cells were cultured in complete DMEM (DMEM with 4.5 g/L glucose supplemented with 10% FBS and 100 U/mL penicillin/streptomycin). To avoid proteolytic cleavage of membrane-bound MICA, we dissociated adherently grown B16F10 cells from the plate using a 0.5 mM EDTA solution (Gibco). EL-4 cells were cultured in complete RPMI 1640 (RPMI 1640 supplemented with 10% FBS and 100 U/mL penicillin/streptomycin). All cells were cultured to maintain optimal densities and kept in a humidified 5% CO_2 incubator at 37°C. Recognition of surface-disposed MICA by the nanobodies was verified by flow cytometry[575].

Expression of the CAR construct was verified by flow cytometry. Briefly, cells were stained with Cy5-conjugated recombinant extracellular MICA*009 (1 μg/mL) for 30 minutes on ice. Cells were washed and viability was determined with LIVE/DEAD™ Fixable Violet Dead Cell Stain Kit (Invitrogen) according to manufacturer's directions. Cells were analyzed on an LSR2 Flow Cytometer (BD Biosciences). Recombinant MICA*009 was produced in-house by transfection of EXPI-293 cells[575].

Mice

C57BL/6J mice and Rag1-deficient mice were purchased from the Jackson Laboratory or bred in-house. Mice were used at 7-12 weeks of age. Experiments were performed in accordance with the guidelines of the Institutional Animal Care and Use Committee (IACUC) of Boston Children's Hospital. Mice were housed under specific pathogen-free conditions in a controlled environment with a 12-hour light-dark cycle and ad libitum access to standard laboratory chow and water. Health status and welfare of the mice were monitored regularly throughout the study.

Design of the VHH CAR construct and virus production

The gene fragments for the CAR were inserted by 'sticky-end' cloning using the BamHI and ClaI restriction enzymes (both from New England Biolabs) into a lentiviral backbone with a mammalian EF-1a promotor (lenti-EF1a-IRES-GFP, a gift from David Williams (Boston Children's Hospital) (Supplementary figure 1). For lentiviral production, we transfected HEK-293T cells with 3µg of CAR plasmid, 2 µg of psPAX2 packaging vector, a gift from Didier Trono (Addgene plasmid #12260; http://n2t.net/addgene:12260; RRID:Addgene_12260) and 1 µg of pMD2.G envelope vector, a gift from Didier Trono (Addgene plasmid #12259; http://n2t.net/addgene:12259; RRID:Addgene_12259) in 500 µl of serum-free DMEM (Gibco). This DNA mixture was added to 100 µl of serum-free DMEM at a 6:1 ratio of FuGENE6 transfection reagent (Promega) and incubated for 15-30 minutes at room temperature. The mixture was then added to ~70% confluent HEK293T cells grown in 10mL of complete DMEM. The medium was replaced ~16 hours after transfection. Lentivirus was harvested 24 and 48 hours after the medium change, the media combined, and concentrated by centrifugation at 45.000xg for 2 hours at 4°C.

Lentiviral transduction and selection of transduced NK-92 cells

NK cells were transduced by centrifugal inoculation. Briefly, $1x10^5$ NK cells were added to a well of a 6-well plate, at a 1:3 ratio of concentrated viral supernatant and complete αMEM. Polybrene infection agent (Sigma-Aldrich) (8 µg/mL) was added to improve transduction. BX795 (1.5 µM), IL-2 (500 IU/mL) and IL-12 (20 ng/mL, all from PeproTech) were added for optimal cell viability. Cells were centrifuged at 2000xg at 30°C, for 90 minutes, resuspended, and incubated in the viral culture medium at 37°C in a humidified 5% CO_2 atmosphere for 4 hours. Centrifugation was repeated at 2000xg at 30°C, for 60 minutes. The medium was then replaced with complete αMEM.

Activation of CAR NK cells by co-culture with MICA-expressing B16F10 cells

WT or MICA-expressing B16F10 or EL-4 cells were incubated at 25,000 cells per well of a 96-well plate together with CAR NK cells at various effector to target ratios in a total volume of 100 µl (1:1 ratio of complete DMEM and complete αMEM) at 37°C in a humidified 5% CO_2 atmosphere. After 24 hours, the IFN-γ concentration in the medium was determined by ELISA, using the human IFN-γ matched antibody pair (Thermofisher scientific) according to the manufacturer's instructions. Cell death was determined with a lactate

dehydrogenase (LDH) Cytotoxicity Assay (Abcam, Ab65393) performed according to the manufacturer's instructions.

CAR NK-92 treatment *in vivo*

$Rag1^{-/-}$ mice were subcutaneously injected in the right flank with $4x10^5$ B16F10 $MICA^+$ cells in PBS. Retro-orbital injections of CAR NK were started on day 3 and treatment injections were given twice weekly at $5\text{-}10x10^6$ cells per injection. Tumor size was measured by calipers and tumor volume was calculated using the formula ($V = 0.5 \times L \times W^2$). Mice were sacrificed once the tumor volume reached $2000mm^3$ or when ulcerations were observed.

PET-CT imaging

To create the imaging agents for PET-CT imaging, we ligated GGG-DFO-Azide to VHH_{188} by sortase-mediated transpeptidation. For sortase reactions, the nanobody was incubated with a 10-fold molar excess of GGG-DFO-Azide and 25 µM Sortase 7M ^{553} overnight at 4°C. Reaction mixtures were depleted of unreacted VHH and Sortase, both containing a C-terminal $(His)_6$-tag on a NiNTA matrix and elimination of free nucleophile by desalting on a PD-10 column (Cytiva), eluting in fractions of 500 µL PBS. We selected and combined fractions 6, 7, and 8 (Supplementary figure 2A). To extend the half-life of the nanobody *in vivo,* the nanobodies were PEGylated by incubation with a 10-fold molar excess of DBCO-PEG20 overnight at 4°C. The reaction was cleaned with a PD-10 column (Cytiva), eluting in fractions of 500 µL PBS. We selected and combined fractions 6, 7, and 8 (Supplementary figure 2B). ^{89}Zr was ordered from the UW-Madison Cyclotron Lab (University of Wisconsin-Madison, USA) and neutralized to a pH of 7.4 by addition of 2M Na_2CO_3 and 1M HEPES. Nanobodies were labeled with ^{89}Zr by DFO-mediated chelation in chelexed PBS and excess, unbound ^{89}Zr was removed by desalting on a PD-10 column and eluted in fractions of 600 µL chelexed PBS (Supplementary figure 3). Radioactivity of the individual fractions was determined and ~60 µCi VHH_{188}-PEG20-^{89}Zr was injected per mouse via retro-orbital injection. Mice were anaesthetized using 2% isoflurane in O_2 at a flow rate of 1 liter per minute. PET/CT scans were obtained 1-, 24-, 48-, and 72-hours post injections on a G8 PET-CT small-animal scanner (PerkinElmer). Each scan had a PET acquisition time of 10 minutes, followed by a CT-scan for 1.5 minutes. PET images were processed and analyzed using VivoQuant software.

Statistical analysis

All statistical analysis was performed with GraphPad Prism 8. Flow cytometry data was analyzed with FlowJo (v10.8.1 and v10.9.0).

Results

Transduction with lentiviral anti-MICA VHH-based CAR constructs yielded stable CAR NK-92 cells

The design of CAR NK cells was based on previously described VHH-based CAR T cells[476] (Figure 1A). We designed a GBlock™ Gene fragment that encodes GFP, followed by a P2A proteolytic processing site to separate the GFP portion from the CAR itself. The CAR antigen recognition domain is encoded by the MICA-specific VHHs A1 or H3, followed by the CD8 hinge and CD8 transmembrane segment and the cytoplasmic signaling and costimulatory domains of CD28 and CD3ζ. The characterization of the anti-MICA VHHs has been described [575]. Cells bearing these VHH-based CARs will be referred to as A1 and H3 CAR NK cells.

As a control, we transduced NK cells with a lentiviral vector containing only a GFP cassette, referred to as empty vector ("EV"). For the NK cells, we observed a low transduction efficiency between 0.3 and 5% (Figure 1B). We therefore sorted the GFP^+ cells to establish a stably transduced cell line. We included a PE channel to eliminate dead auto-fluorescent cells that show up in the PE channel. Flow cytometry performed on the H3 CAR NK cells shows the presence of two distinct populations of GFP^+ cells, attributed to the combination of two cell lines transduced on separate days, done to obtain adequate numbers of cells (Figure 1C). To verify CAR surface expression, we stained the CAR NK cells with Cy5-conjugated MICA protein, which binds to the extracellularly exposed nanobodies that are part of the CAR. Flow cytometry produced a clear signal in the Cy5 channel for the A1 CAR NK cells, showing surface expression of the VHH-A1 based CAR. We saw a weak signal in the Cy5 channel for the H3 CAR NK cells, indicating weaker expression of the VHH-H3 based CAR (Figure 1D).

For the H3 CAR NK cells, both the GFP^{hi} and the GFP^{lo} population show the same signal in the Cy5 channel (supplementary figure 4). Immunoblots prepared with anti-CD3ζ antibodies (signal at 40 kD in A1 and H3 CAR NK cells) showed expression of the CAR. The GFP polypeptide produced by the Lenti-EF1α A1 and H3 NK cell lysates migrates slightly higher on SDS -PAGE than the GFP produced by the Lenti-EF1a empty vector, attributable to the continued presence of the P2A peptide sequence downstream of the GFP in the CAR construct (Figure 1E). Gating for flow cell sorting and flow cytometry is shown in supplementary figures 5-7.

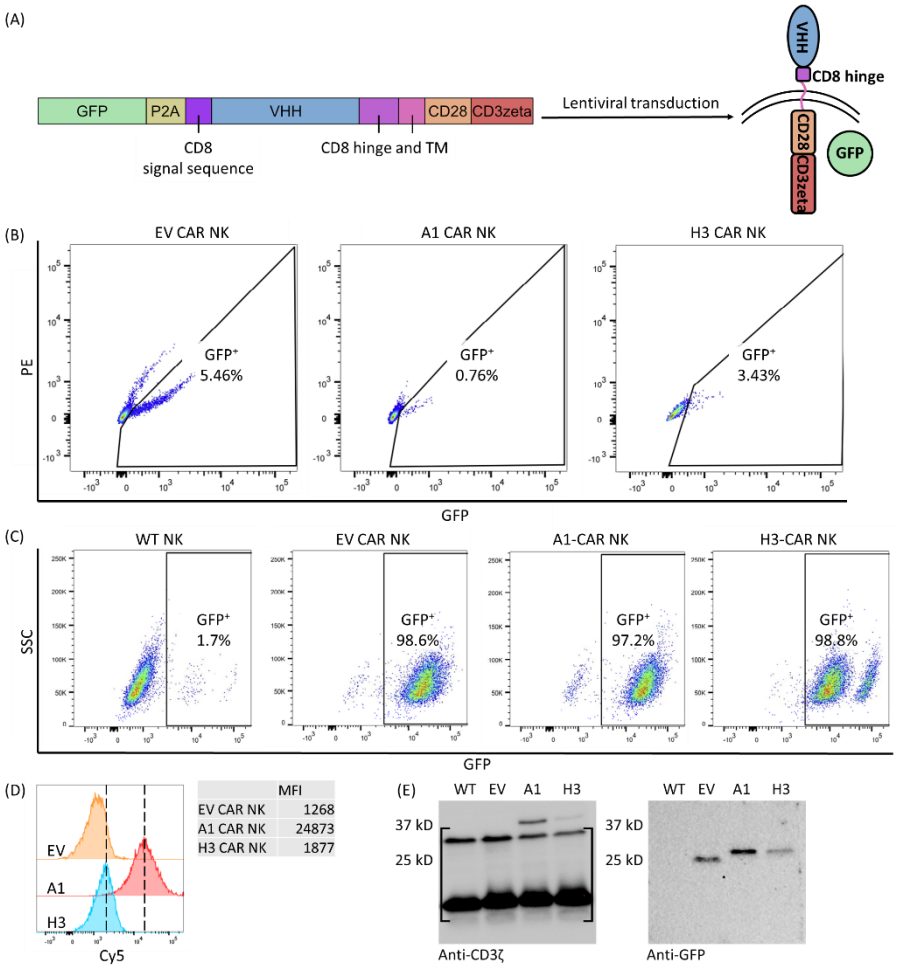

Figure 1. The production and establishment of stable CAR NK cells. *(A) Schematic overview of the CAR construct as transduced into NK cells. We used a lentiviral backbone with a mammalian EF1a promotor and incorporated the sequences of either VHH A1 or VHH H3, the costimulatory and activation signals of CD28 and CD3ζ, and GFP separated from the rest of the construct by a P2A peptide cleavage signal. Construct maps for A1 CAR NK, H3 CAR NK and EV CAR NK are shown in supplementary figure 1. (B) After transduction, GFP positive cells were deemed to be transduced successfully, and therefore sorted by FACS. We included a PE channel to eliminate dead, auto-fluorescent cells. Gating shown in supplementary figure 5. (C) We continually monitored GFP expression in the CAR NK cells and found a stable expression after at least 4 months in culture, with a GFP positive population of 98.6% for the EV NK cells, 97.2% for the A1 CAR NK cells, and 98.8% for H3 CAR NK cells. Gating shown in supplementary figure 6. LEGEND CONTINUES ON THE NEXT PAGE.*

(D) To verify CAR surface expression by flow cytometry, we stained the CAR NK cells with Cy5-conjugated recombinant MICA protein. We observed a clear signal in the Cy5 channel for the A1 CAR NK cells, thus establishing surface expression of VHH-A1 as part of the CAR. We saw a weak signal in the Cy5 channel for the H3 CAR NK cells, indicating weaker expression of the VHH-H3-bearing CAR. Gating is shown in supplementary figure 7. (E) Immunoblots prepared with anti-CD3ζ antibodies showed expression of the actual CAR portion of the viral vector with a signal at 40 kD in A1 and H3 CAR NK cells and an absence of signal in WT and EV CAR NK cells. The GFP polypeptide produced by the Lenti-EF1α A1 and H3 NK cell lysates runs slightly higher than that of GFP produced by the Lenti-EF1a empty vector cell lysate, which we attribute to the presence of the P2A peptide sequence downstream of the GFP in the CAR construct. The weaker signal observed for the H3 CAR NK cells matches that observed by flow cytometry. The signal in brackets is non-specific.

MICA-expressing tumor cells activate A1 and H3 CAR NK-92 cells and elicit cytotoxicity

Because mice lack a protein homologous to human MICA, we used MICA transfectants of the mouse-derived B16F10 melanoma (MICA*009) and EL-4 T cell lymphoma (MICA*008) lines. We incubated A1 and H3 CAR NK cells with WT or MICA$^+$ B16F10 cells or with WT or MICA$^+$ EL-4 cells. We co-cultured effector cells and target cells at different ratios ([1:1], [0.2:1] and [0.1:1]), keeping the number of target cells constant and varying the number of effector cells. For the A1 and H3 CAR NK cells, at all [E:T] ratios, we observed a significant increase in cell death of MICA$^+$ cells as measured by LDH release. Co-culture of MICA$^+$ cells with EV CAR NK cells showed no such increase in cytotoxicity. No cytotoxicity was observed when co-culturing WT B16F10 cells with the A1 or H3 CAR NK cells. We observed a significant increase in cytotoxicity of EL-4 MICA$^+$ cells co-cultured with A1 CAR NK cells or H3 CAR NK cells when compared to cytotoxicity exerted by EV CAR NK cells. No significant increase in cytotoxicity was observed in WT EL-4 cells co-cultured with EV, A1, or H3 CAR NK cells (Figure 2A).

To relate this cytotoxicity to activation of CAR NK cells, we measured IFNy secretion by ELISA. Upon co-culture with B16F10 MICA$^+$ we observed an increase in IFNy secretion for the A1 and H3 CAR NK cells, but not for the EV CAR NK cells. CAR NK cells co-cultured with B16F10 WT cells showed no such increase. We observed an increase in IFNy expression when A1 CAR NK cells were co-cultured with EL-4 MICA$^+$ cells at [1:1], but not for any of the other conditions, despite the observed significant difference in cytotoxicity (Figure 2B). We attribute this to the fact that we observed lower MICA expression levels on the surface of the EL-4 MICA$^+$ cells compared to the B16F10 MICA$^+$ cells[575]. Furthermore, EL-4 cells are suspension cells, while

B16F10 cells are adherent, potentially facilitating an interaction with NK cells. These results indicate the possibility of CAR NK cells to treat MICA positive tumors *in vivo*.

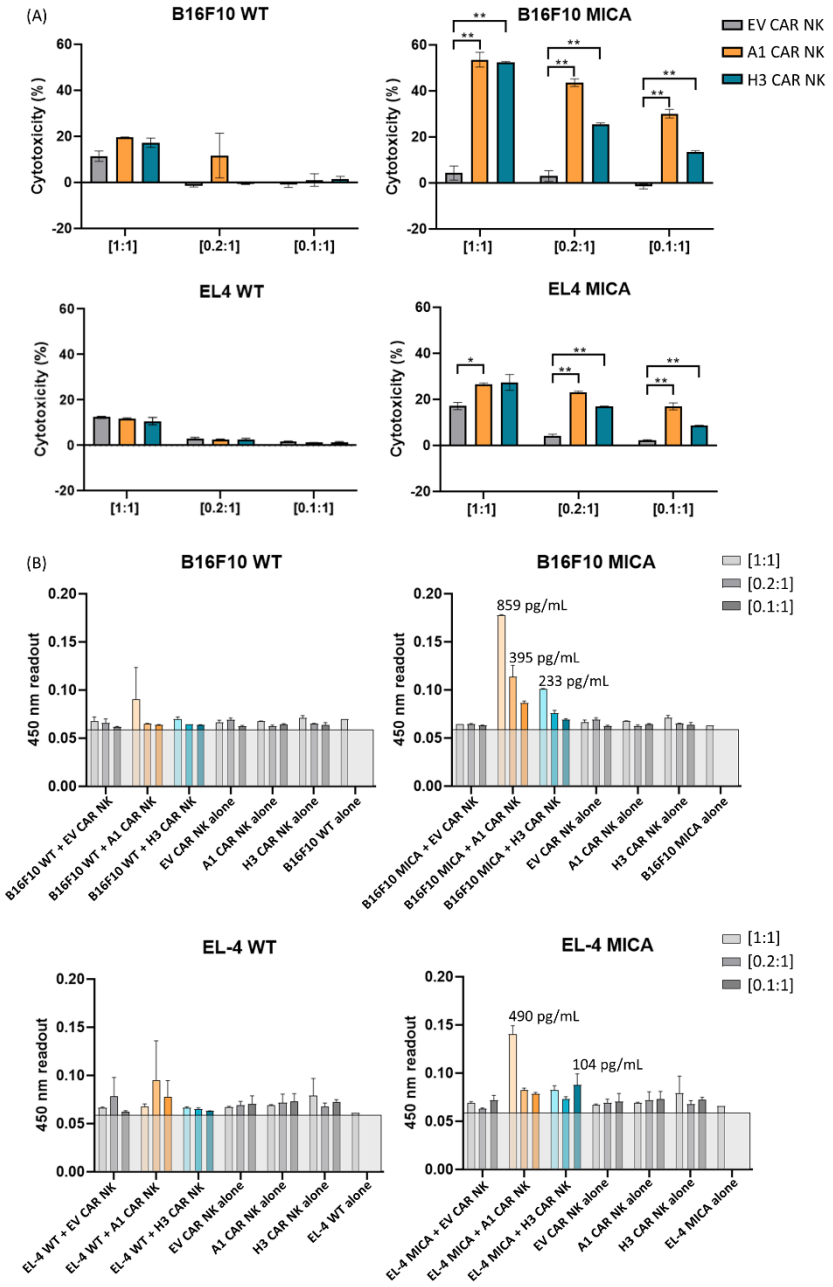

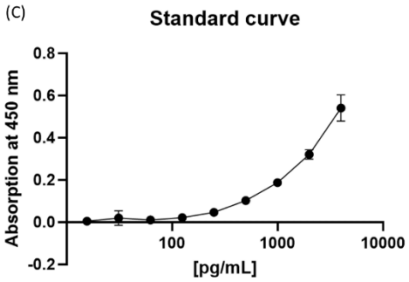

Figure 2. In vitro cytotoxicity of CAR NK cells co-cultured with MICA⁺ targets. *We incubated EV, A1, and H3 CAR NK cells with WT B16F10 or EL-4 cells, or B16F10 or EL-4 cells that stably express MICA. We incubated at effector to target ratios [E:T] of [1:1], [0.2:1], or [0.1:1], keeping the number of target cells consistent and varying the number of effector cells. (A) 24 hours after co-culture, cytotoxicity was determined by measuring LDH release in the medium. Cytotoxicity percentages were normalized to target cells without CAR NK co-culture as a background control (0% cell death), or lysed target cells as a high control (100% cell death). We observed a significant increase in cytotoxicity of B16F10 MICA⁺ cells co-cultured with A1 CAR NK cells and H3 CAR NK cells compared to EV CAR NK cells at all [E:T] ([1:1] p = 0.004 for A1; p = 0.002 for H3, [0.2:1] p = 0.0024 for A1; p = 0.0055 for H3 and [0.1:1] p = 0.0022 for A1; p = 0.0027 for H3). EL-4 MICA⁺ cells showed a lower overall cytotoxicity of 15-30% when co-cultured with A1 and H3 CAR NK cells. We observed a significant increase in cytotoxicity of EL-4 MICA⁺ cells co-cultured with A1 CAR NK cells or H3 CAR NK cells compared to EV CAR NK cells at most [E:T] ([1:1] p = 0.015 for A1; p = 0.061 for H3, [0.2:1] p = 0.0011 for A1; p = 0.0016 for H3, [0.1:1] p = 0.0055 for A1; p = 0.0014 for H3). No significant increase in cytotoxicity was observed when WT cells were co-cultured with EV, A1, or H3 CAR NK cells. (B) After 24 hours of co-culture, the concentration of IFNγ in the medium was determined by sandwich ELISA with a matched human IFNγ antibody pair. We observed a significant increase in IFNγ secretion in the A1 and H3 CAR NK cells, but not in EV CAR NK cells, when co-cultured with B16F10 MICA⁺. We show the raw values of the ELISA plate read-out at 450 nm and the estimated IFNγ production in pg/mL by extrapolation from the standard curve (C).*

MICA⁺ tumor-bearing mice treated with A1 CAR NK-92 cells show reduced tumor growth and increased survival probability

We inoculated RAG1$^{-/-}$ mice with 4x10^5 B16F10 MICA⁺ cells via subcutaneous injection. Twice weekly, we treated the mice with EV CAR NK cells (n = 3) or A1 CAR NK cells (n = 7) by retro-orbital injection for a total of 5 injections and followed tumor growth by caliper measurements (Figure 3A). Mice treated with A1 CAR NK cells show a significant delay in tumor growth compared to mice treated with EV CAR NK cells (p = 0.0075) (Figure 3B). Furthermore, mice treated with A1 CAR NK cells showed a significant increase in survival probability (p = 0.0011) (Figure 3C). Of the mice treated with EV CAR NK

cells, one mouse was euthanized on day 17 because of severe ulcerations. Two mice were euthanized on day 17 and 18 when the tumor volume exceeded 2000mm^3. Of the mice treated with A1 CAR NK cells, one mouse was euthanized on day 20 and one on day 21, both because of severe ulcerations. All other mice were euthanized when the tumor volume exceeded 2000 mm^3. These results support the possibility of nanobody-based CAR NK cells to treat MICA$^+$ tumors.

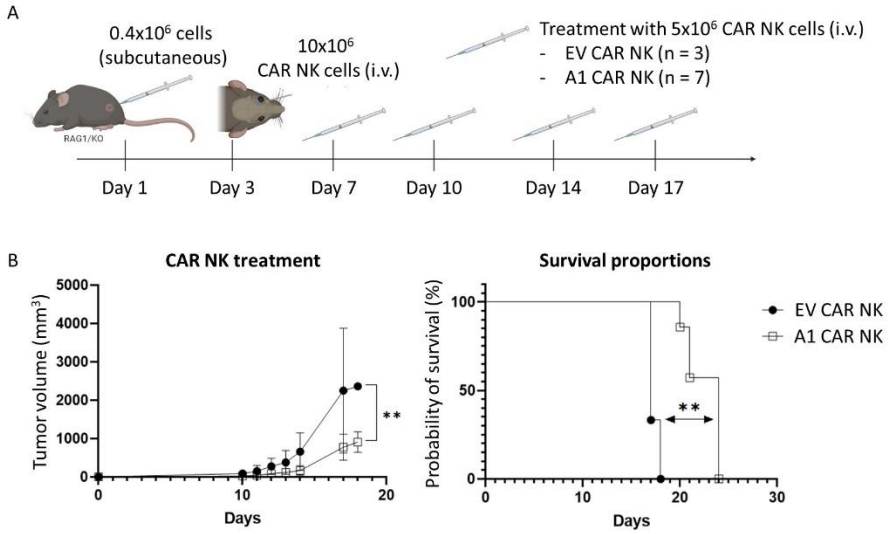

Figure 3. In vivo cytotoxicity of CAR NK cells in MICA$^+$ tumor-bearing mice. *(A) We challenged RAG1/KO mice with B16F10 MICA cells by subcutaneous injection. On day 3 post tumor graft, we treated the mice with a retro-orbital dose of 10x10^6 CAR NK cells and reduced the dose to 5x10^6 cells per mouse for the treatments twice weekly thereafter. (B) Mice treated with A1 CAR NK cells show a significant delay in tumor growth compared to mice treated with EV CAR NK cells (p = 0.0075) (Calculated with two-way ANOVA). (C) Mice treated with A1 CAR NK cells showed a significant increase in survival probability (p = 0.0011) (Calculated with the Mantel-Cox test).*

Immuno-PET traces CAR NK-92 cells to MICA$^+$ tumors

To track the localization of CAR NK cells to MICA$^+$ tumors, we inoculated C57/B6 mice with B16F10 MICA$^+$ tumors by tail vein injection and allowed lung metastases to form for 15 days. We used PEGylated ^{89}Zr-labeled VHH$_{188}$ (Supplementary figure 2), a nanobody that targets the human transferrin receptor on the NK cells, which are of human origin (Supplementary figure 8) for immuno-PET imaging. VHH$_{188}$ does not recognize the mouse transferrin receptor [601]. On day 1 of imaging, mice were injected with either EV CAR NK cells or A1 CAR NK cells (both 5x10^6 cells/mouse) into one retro-orbital cavity,

and ^{89}Zr-labeled PEGylated VHH_{188} (60 µCi/mouse) into the other retro-orbital cavity.

We were able to localize the CAR NK cells to the lungs of the mice that received B16F10 MICA$^+$ tumors up to 72 hours after NK cell injection (Figure 4B). We observed slightly more positive nodules in the lungs of the mice that received A1 CAR NK cells compared to EV CAR NK cells at 72 hours post-injection, although it is difficult to draw a meaningful conclusion based on these small differences, seen only at the 72-hour timepoint. Possibly the EV CAR NK are cleared from the circulation more rapidly, due to their inability to bind to a MICA target. Upon dissection of the lungs, we saw clear metastatic lesions on the surface of the lungs (Figure 4C). The resolution of the PET images used is ~1.4 mm, which makes it difficult to visualize positive signal in greater detail.

Discussion

MICA and MICB are Class I MHC-related proteins expressed on stressed and cancerous cells. Their presence can serve not only as a diagnostic marker of malignancies, but also as a possible target for therapy. While typical immunoglobulins exert their functional properties through Fc effector functions, their size compromises efficient tissue penetration. Nanobodies offer an appealing alternative to immunoglobulins for the purpose of launching an immune attack on MICA-positive tumors. We previously produced high affinity nanobodies, A1 and H3, that recognize the extracellular portion of MICA, alleles *008 and *009, on the surface of MICA$^+$ B16F10 melanoma cells and MICA$^+$ EL-4- T-cell lymphoma cells.

Adoptive cell transfer is widely explored as a possible cancer therapy. The success of VHH-based CAR T cells in tumor treatment has been recorded[476], with the first VHH-based CAR T cell therapy (Carvykti) approved for treatment of relapsed or refractory multiple myeloma[602]. Despite the success of CAR T cells, significant drawbacks and side-effects deserve consideration. T cells are often sourced from the patient's own peripheral blood and require expansion *ex vivo* after modification. CAR NK cells can be obtained from a wider range of sources, such as the patient's or a donor's peripheral blood, from placenta or umbilical cord blood, existing immortalized NK cell lines (NK-92) or manufactured from induced pluripotent stem cells (iPSC)[205–210].

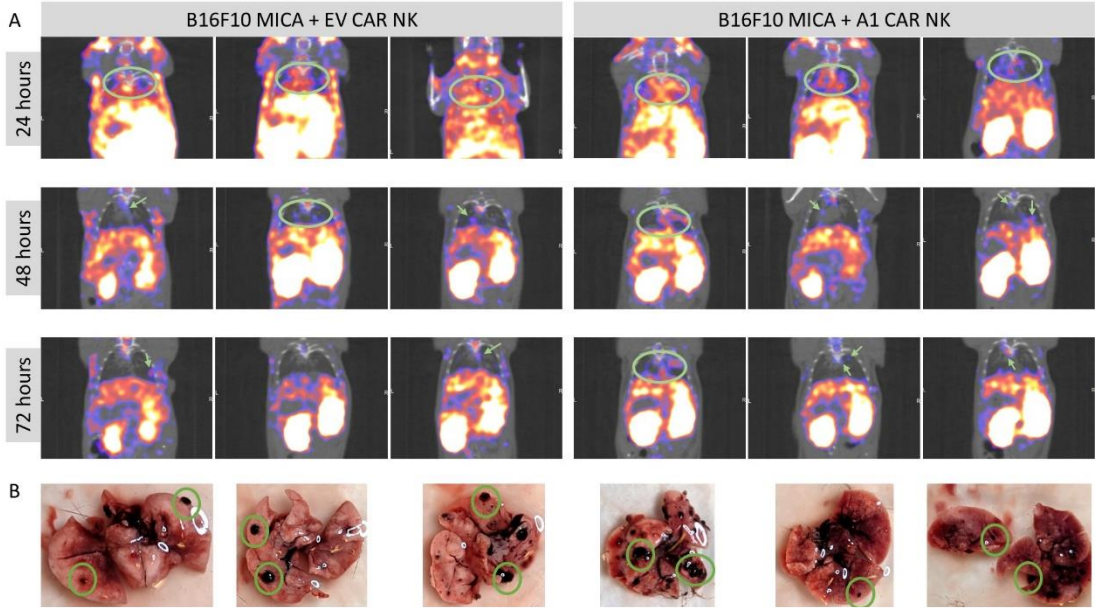

Figure 4. PET imaging to track localization of CAR NK cells to MICA⁺ lung metastases. *(A) We injected C57/Bl6 mice with B16F10 MICA⁺ cells by tail vein injection and allowed metastases to form for 15 days. On day 1 of imaging, EV and A1 CAR NK cells and ^{89}Zr-VHH$_{188}$ were injected retro-orbitally. We were able to localize the A1 CAR NK cells to the lungs of the mice that received B16F10 MICA⁺ tumors up to 72 hours after NK cell injection (circles and arrows). Little if any signal remained at the 72-hour timepoint for mice that received EV CAR NK cells. Regardless of the type of CAR NK cells transferred, strong PET signals were seen in the liver. In grayscale: CT density in HU (Houndsfield units), in color: PET intensity in Bq/mL. Coronal sections through the lungs are shown. For full images and intensity scales, see supplementary figure 9. For 3D videos, see 10.6084/m9.figshare.25471795. (B) We dissected the lungs of each mouse and observed metastases on the lung surface (several highlighted by circles).*

A major reported side effect of CAR T therapy is cytokine release syndrome (CRS), a systemic inflammation caused by excessive secretion of cytokines such as IL-2 and IL-6 released by the CAR T cells. Other immune cells may respond to cytokines produced by the CAR T cells and also contribute to pathology. Most of the cytokines released by NK cells (IL-3, and TNF-α) do not induce such inflammation, and thus are less likely to cause CRS[217], although CRS due to overexpression of IFN-γ has been reported in a patient receiving CAR NK cells, thus careful monitoring is still required[603]. For these reasons, CAR NK cell therapy is potentially a more effective and safer alternative to CAR T cell therapy.

Here, we developed VHH_{MICA}-based CAR NK cells that target and selectively kill $MICA^+$ B16F10 and $MICA^+$ EL-4 cells *in vitro*. Immuno-PET shows that the A1 CAR NK cells localize to the lungs of mice bearing $MICA^+$ B16F10 lung metastases. We see such localization until 72 hours post injection. The CAR NK cells are also cytotoxic towards $MICA^+$ B16F10 cells *in vivo*. $MICA^+$ B16F10 tumor-bearing mice treated with A1 CAR NK cells show a significant reduction in the rate of tumor growth and increase in overall survival compared to mice treated with EV CAR NK cells.

We recognize the limitation of using mouse-derived cancer cells that have been rendered MICA-positive by transfection. A major constraint is the availability of patient-derived cancer cell lines that not only express the correct alleles of MICA but that are also suitable for transplantation. Using such lines for engraftment of immunocompetent mice poses a risk of a possible xenogeneic response independent of MICA expression, and thus requires the use of immunodeficient recipients.

Although MICA is generally absent from healthy tissue, expression of MICA is seen in gut epithelium, although primarily intracellularly[604,605]. Since gut epithelia are capable of rapid repair, this risk may be manageable, should MICA-specific CAR NK cells indeed attack gut epithelia. Nevertheless, since mice do not possess a MICA homolog, the use of MICA-transgenic mice[606] might allow an assessment of any "off-tumor, on-target" effects when using MICA-targeting CAR NK cells.

The genetic instability of NK-92 cells requires their irradiation prior to infusion in a patient, which impairs their proliferation and limits their persistence *in vivo*[607]. Patient-specific induced pluripotent stem cell-derived NK cells (iPSC-NKs) may be better for CAR T and CAR NK cell therapy.

iPSC-NK cells express the CD16 Fc receptor and are thus capable of antibody-dependent cellular cytotoxicity (ADCC)[207,608–610].

Despite excellent results in the treatment of certain hematological cancers, the efficiency of CAR treatment in solid tumors remains poor. The CARs used in this study are based on what is referred to as a "second-generation" CAR, which includes a CD3ζ signaling domain and CD28 co-stimulatory domain. Possible improvements to this CAR design include the addition of a cytokine auto-stimulation domain, such as IL-15[611,612]. Third- and fourth-generation CARs employ additional co-stimulatory domains such as CD27 or STAT3/5 binding motifs. Other modifications, such as enhanced CD28 signaling domains or the inclusion of ITAMs 2 and 3 in CD3ζ may increase the stability of CAR cells and thus show better tumor control *in vivo*[613].

The tumor microenvironment often shows deposition of extracellular matrix (ECM) components and may cause encapsulation of a solid tumor that limits access to the tumor for CAR T or CAR NK cells. Instead of CAR T or CAR NK cells, MICA-specific CAR macrophages might help degrade the ECM by secretion of proteases and improve the outcome of immunotherapy[614–619]. Because VHH A1 and VHH H3 recognize different epitopes on MICA[575], we could use H3-based CAR macrophages to help degrade the ECM and attract A1-based CAR NK cells to aid in tumor-specific cytotoxicity, without the different cell types competing for binding to MICA.

Conflict of Interest

The authors declare that the research was conducted in the absence of any commercial or financial relationships that could be construed as a potential conflict of interest.

Author Contributions

The authors confirm their contribution to the paper as follows: E.R.V and H.L.P designed the study and supervised data collection. E.R.V and W.v.K designed and produced the CAR NK cells. E.R.V and A.K. performed research with the CAR NK cells. T.B provided guidance on PET imaging and the work with the anti-transferrin receptor nanobody. E.R.V. and H.L.P. wrote the paper. All authors reviewed the results and approved the final version of the manuscript.

Acknowledgments

This research was supported by the NIH Pioneer Grant (DP1AI150593-05). T.B. was supported by fellowships from the Belgian American Educational Foundation and from Wallonie-Bruxelles International (WBI.World). We

gratefully acknowledge Dr. Maarten Dewilde (KU Leuven) and Dr. Bart De Strooper (KU Leuven) for providing VHH188. We gratefully acknowledge Dr. Ryan Alexander for helpful discussions regarding the CAR NK production, Dr. Xin Liu for helpful discussions and performing tail vein injections in mice, and Claire Carpenet, MSc, for guidance with PET imaging and PET imaging data analysis.

Data availability

All data is included in the manuscript and supporting information. 3D videos of PET/CT imaging available at 10.6084/m9.figshare.25471795. All data underlying this publication, including but not limited to raw data, designs, diagrams, data files, statistical records, unique materials, graphs, and other research data will be available upon request.

Supplementary figures

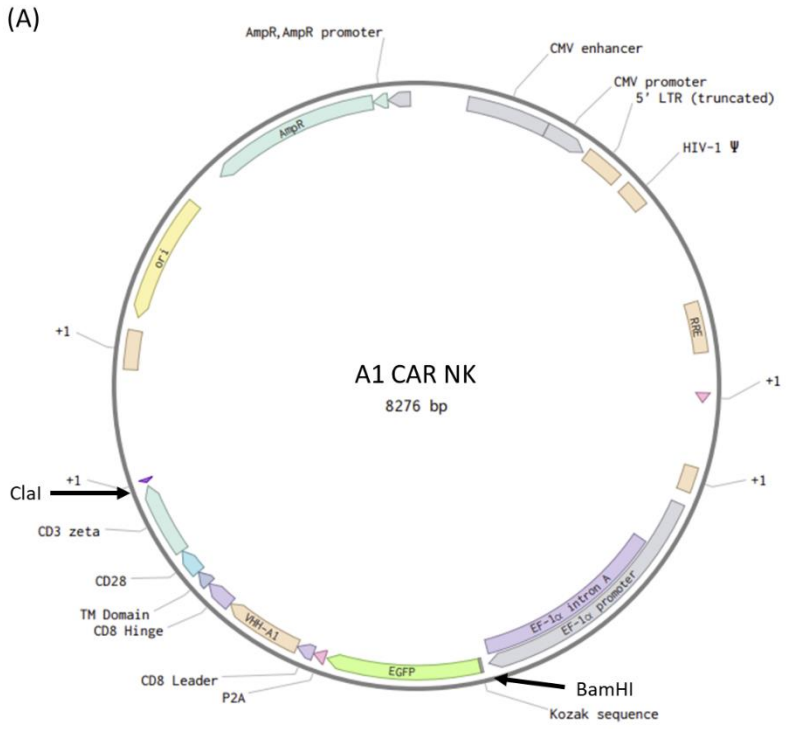

(B)

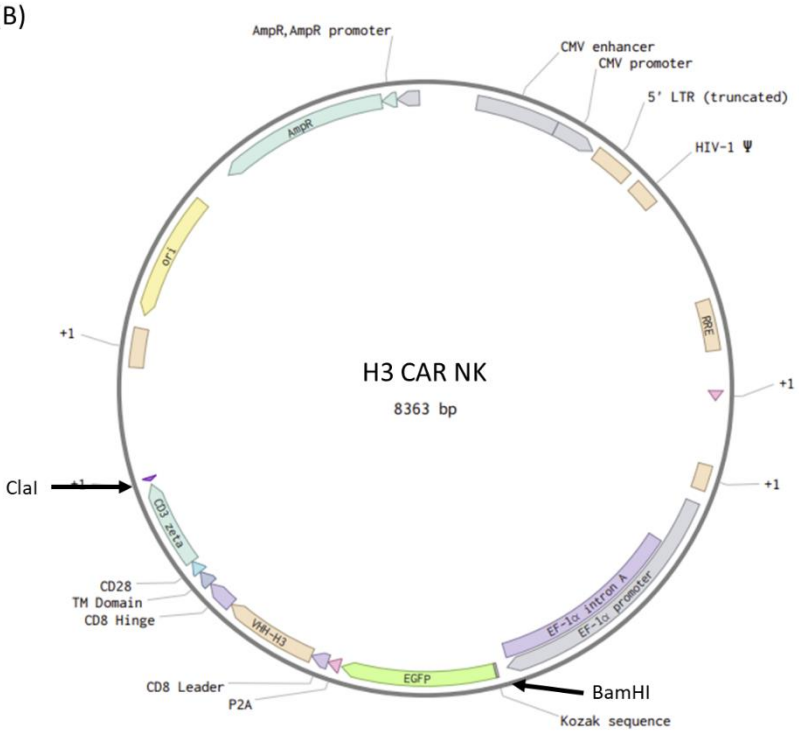
AmpR, AmpR promoter
CMV enhancer
CMV promoter
5' LTR (truncated)
HIV-1 Ψ
RRE
+1
+1
+1
EF-1α Intron A
EF-1α promoter
BamHI
Kozak sequence
EGFP
P2A
CD8 Leader
VHH-H3
CD8 Hinge
TM Domain
CD28
CD3 zeta
ClaI
ori
AmpR
H3 CAR NK
8363 bp

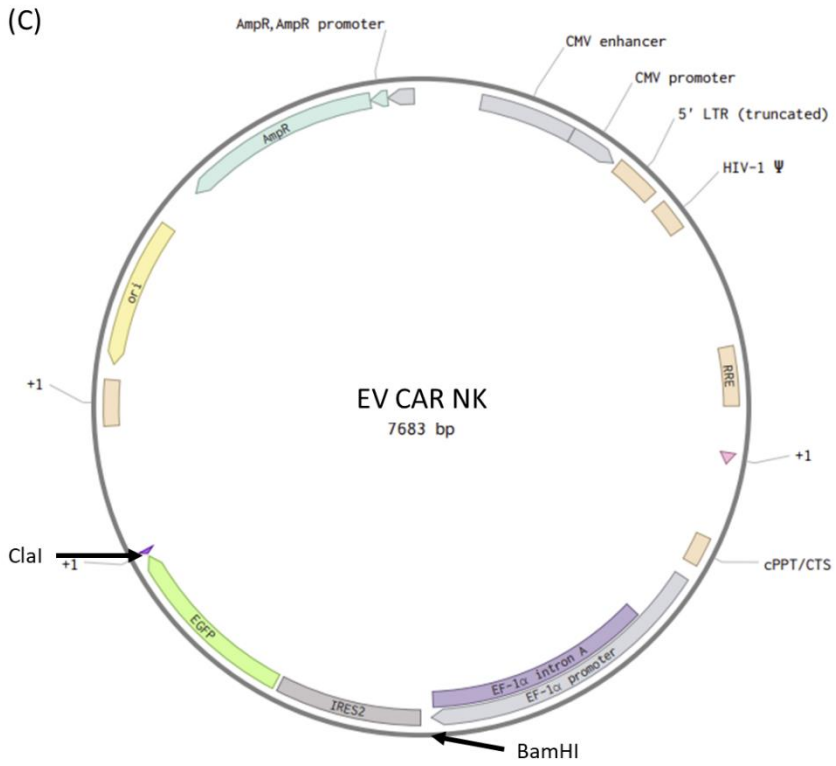

Supplementary figure 1. Lentiviral vector maps used for the transduction of NK-92 cells. *We designed a GBlock™ gene fragment that encodes for EGFP, followed by a P2A proteolytic processing site separating the EGFP from the CAR. The CAR antigen recognition domain is encoded by the amino acid sequence of VHH A1 (A) or VHH H3 (B), separated by a CD8 hinge from the transmembrane segment and the cytoplasmic signaling and costimulatory domains of CD28 and CD3ζ. The gene fragments were inserted into a Lentiviral backbone with the mammalian EF-1α promotor by 'sticky-end' cloning using the BamHI and ClaI restriction enzymes (both from New England Biolabs). For the empty vector (EV) CAR NK-92 cells, we transduced NK-92 cells with the unmodified lentiviral vector containing only the EGFP cassette (C).*

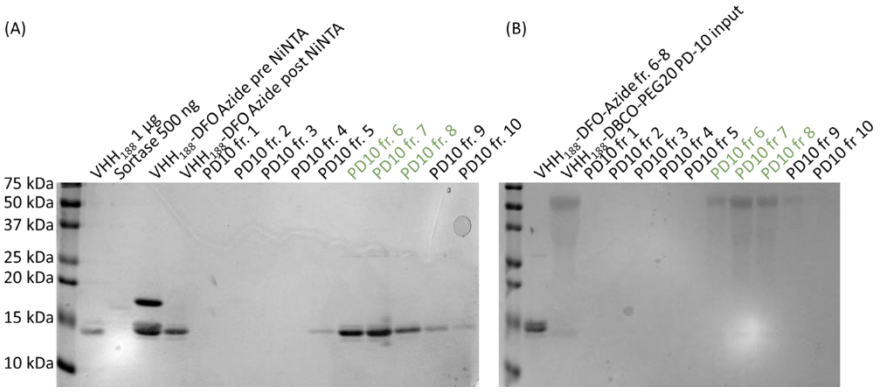

Supplementary figure 2. Preparation of VHH$_{188}$-DFO-PEG20 for labeling with 89Zr to be used in PET imaging. *(A) We installed DFO-Azide on VHH$_{188}$, a nanobody targeting the human transferrin receptor found on the NK cells, with a sortase reaction. The reaction was depleted of unreacted nanobody and sortase, both containing a (His)$_6$-tag, on a NiNTA matrix. The reaction was depleted of unreacted DFO-Azide using a PD-10 desalting column. (B) Fractions 6, 7, and 8 were used to install DBCO-PEG20 on the nanobody by means of a click-reaction between the DBCO and Azide. The reaction was depleted of unreacted DBCO-PEG20 with a PD-10 desalting column. Fractions 6, 7, and 8 were combined for labeling with ^{89}Zr.*

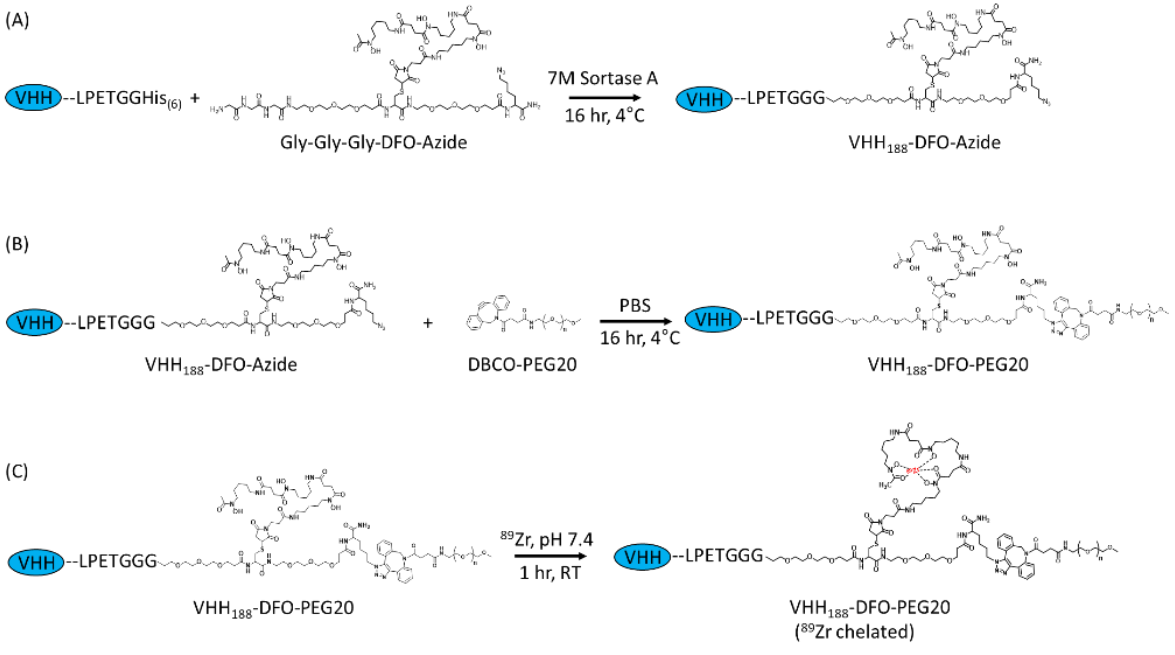

Supplementary figure 3. Schematic overview of the production of VHH_{188}-PEG20-^{89}Zr. *(A) We ligated GGG-DFO-Azide to VHH_{188} by sortase-mediated transpeptidation. We incubated the nanobody, containing a C-terminal LPETGG sortase motif and $(His)_6$-tag, with a 10-fold molar excess of GGG-DFO-Azide and 25 µM " 7M Sortase A, overnight at 4°C. The reaction mixture was depleted of unreacted VHH and Sortase, both containing a C-terminal $(His)_6$-tag, on a NiNTA matrix. Free nucleophile was eliminated by desalting on a PD-10 column. (B) To extend the half-life of the nanobody in vivo, the nanobodies were PEGylated by incubation with a 10-fold molar excess of DBCO-PEG20 overnight at 4°C. (C) ^{89}Zr was neutralized to a pH of 7.4 by addition of 2M Na_2CO_3 and 1M HEPES. Nanobodies were labeled with ^{89}Zr by DFO-mediated chelation in chelexed PBS.*

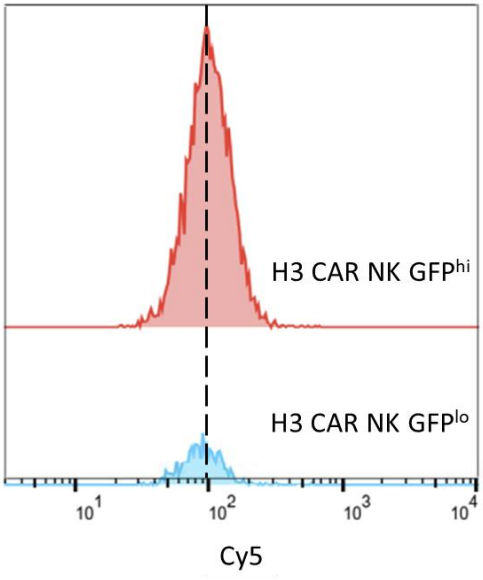

Supplementary figure 4. H3 CAR NK Cy5 expression based on dividing the CAR NK cells in a GFP^{hi} and GFP^{lo} population. *We stained cells with Cy5-conjugated recombinant MICA (1 µg/mL) for 30 minutes on ice. We determined viability with LIVE/DEAD Cell stain (1:200). Both populations show similar signal in the Cy5 channel.*

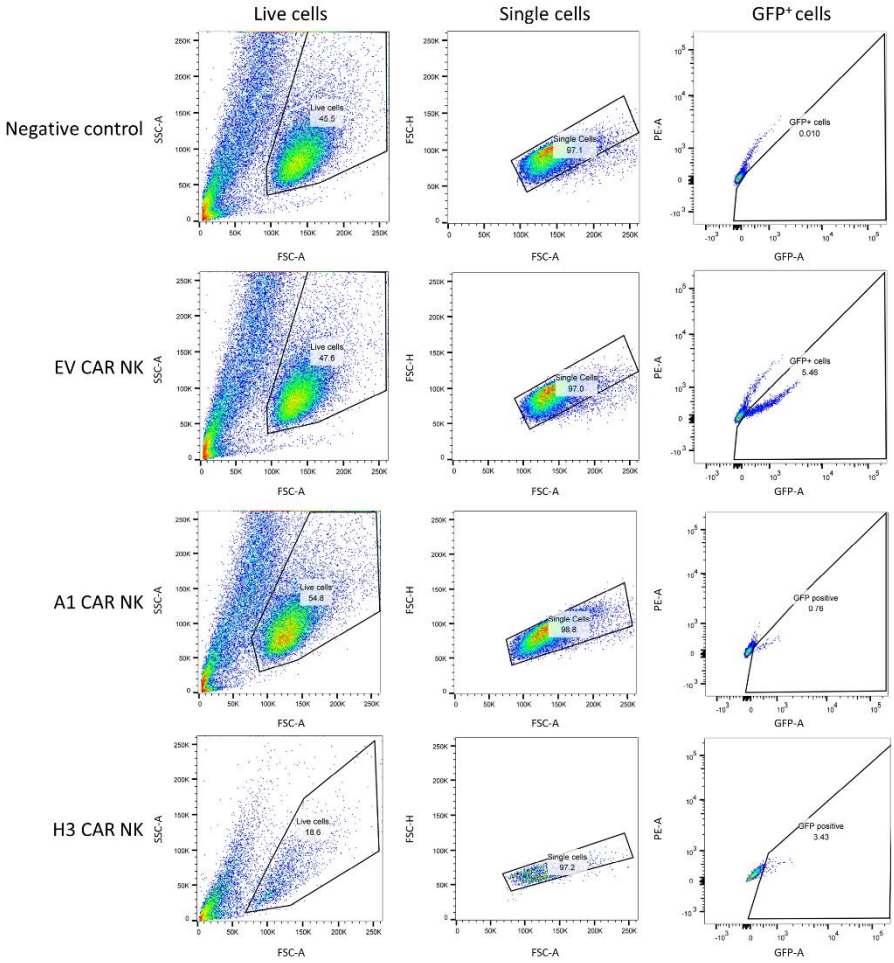

Supplementary figure 5. Gating strategy for the sorting of CAR NK-92 cells. *Due to transduction on different days all cell lines (EV, A1, and H3 CAR NK-92) were sorted on different days, but we used comparable gating for all samples. A negative (untransduced) control was added for each sample, here the negative control used for sorting of EV CAR NK-92 cells is shown. First, we gated on live cells determined by FSC and SSC. Next, we gated on singlets, determined by FSC-H and FSC-A. We sorted the GFP-positive cells based on a gate set for the negative (untransduced) control cells.*

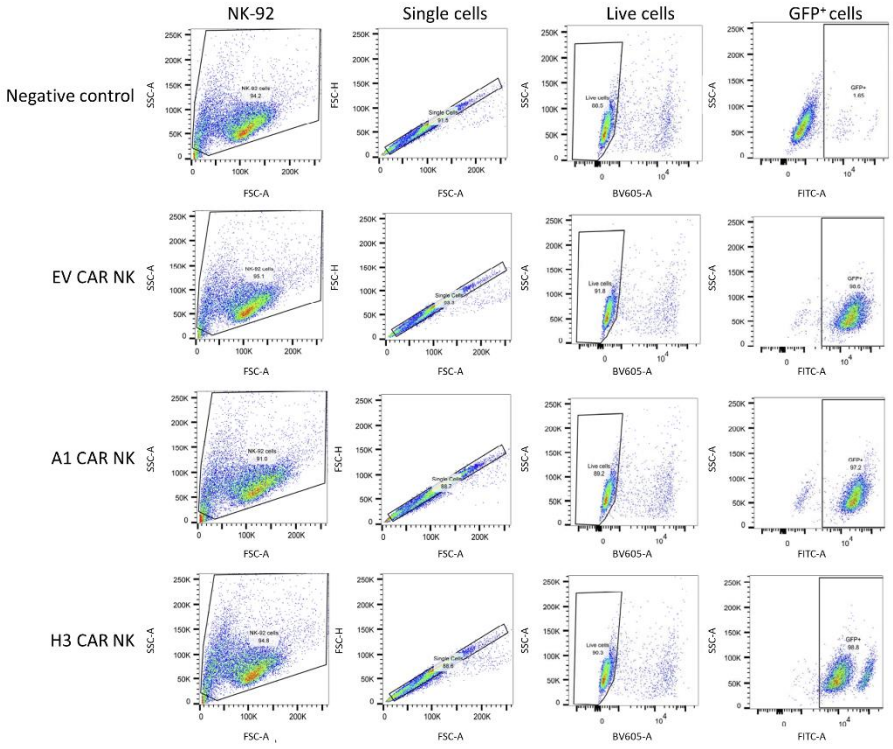

Supplementary figure 6. Gating strategy for determining stability of sorted CAR NK-92 cells. *A negative (untransduced) control was used to determine the GFP-negative population. Cells were stained with propidium iodide to determine viability. First, we selected the cells based on FSC and SSC. Next, we gated on singlets, determined by FSC-H and FSC-A. We measured GFP expression in the FITC channel on live cells, which stain negative in the BV605 channel.*

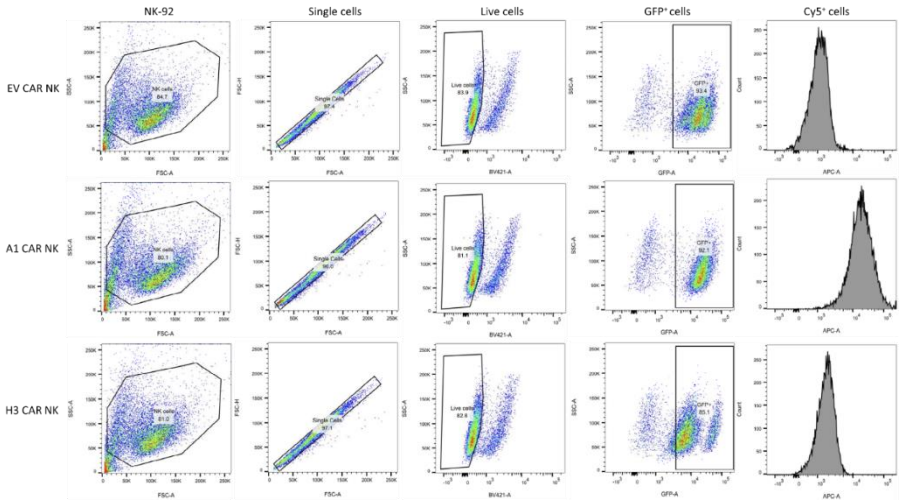

Supplementary figure 7. Gating strategy for determining extracellular expression of nanobody-based CAR construct. *We stained cells with Cy5-conjugated recombinant MICA (1 µg/mL) for 30 minutes on ice. We determined viability with LIVE/DEAD Cell stain (1:200).*

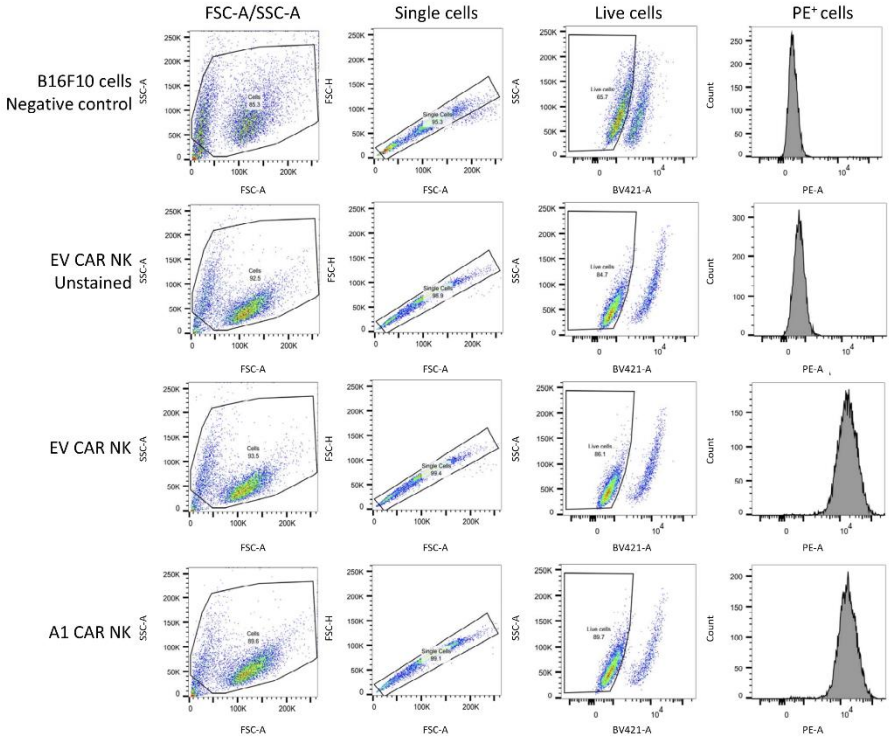

Supplementary figure 8. Gating strategy for determining human transferrin receptor staining with VHH_{188} on CAR NK-92 cells. *We stained cells with biotinylated anti-transferrin receptor nanobody VHH_{188} (1 µg/mL) and streptavidin-conjugated PE (2.5 µg/mL) and determined viability with LIVE/DEAD Cell stain (1:200). To ensure a positive signal is from binding of VHH_{188}, a control stained with only Strep-PE and viability dye was added for both cell lines (shown here for EV CAR NK-92). A murine B16F10 cell line, which should stain negative with VHH_{188}, was added as negative control. First, we selected the cells based on FSC and SSC and gated these cells on singlets, determined by FSC-H and FSC-A. We selected live cells that stained negative in the BV421 channel. We measured human Transferrin-receptor staining in the PE channel.*

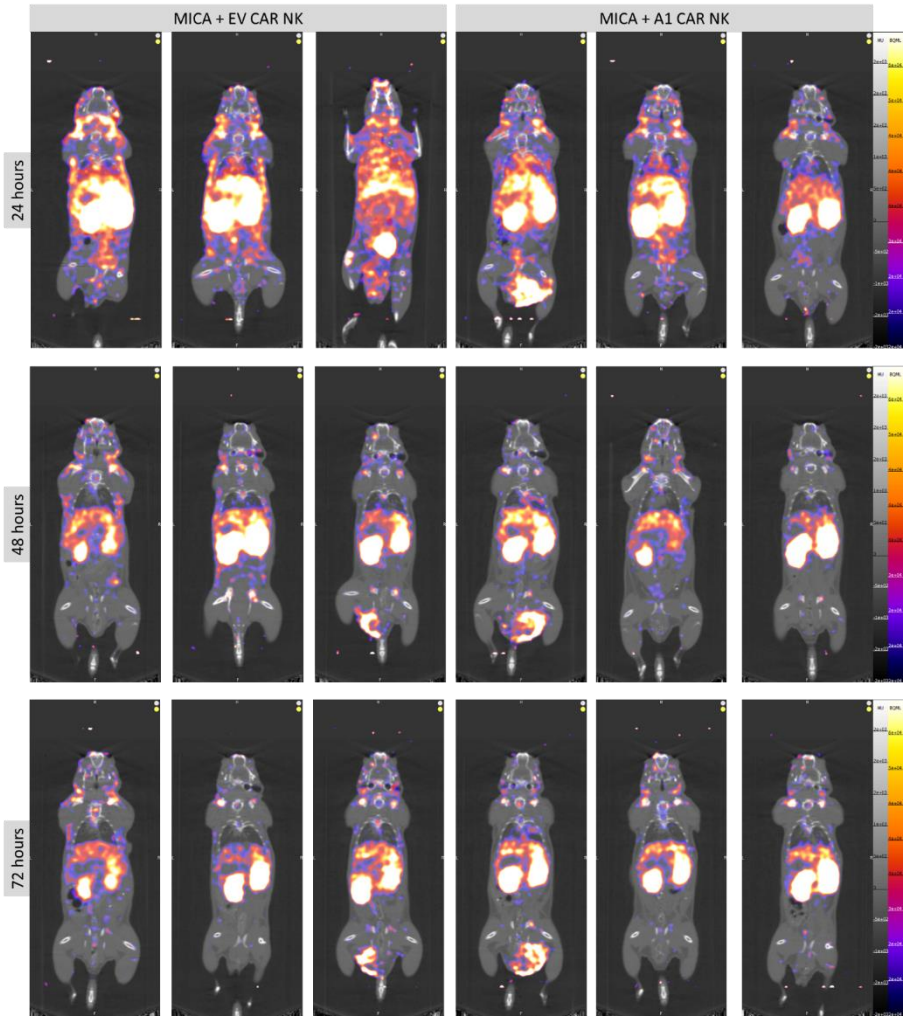

Supplementary figure 9. Full-body immuno-PET images with ^{89}Zr-labeled VHH$_{188}$ of mice injected with EV CAR NK or A1 CAR NK at t = 24 hours, 48 hours, and 72 hours after injection. *Coronal sections through the lungs are shown here. In grayscale: CT density in HU (Houndsfield units), in color: PET intensity in Bq/mL.*